EPJ manuscript No.
(will be inserted by the editor)

Total photoproduction cross-section at very high energy

R.M. Godbole[1], A. Grau[2], G. Pancheri[3], and Y.N. Srivastava[4]

[1] Centre for High Energy Physics, Indian Institute of Science, Bangalore, 560012, India.
[2] Departamento de Física Teórica y del Cosmos and CAFPE, Universidad de Granada, 18071 Granada, Spain.
[3] INFN Frascati National Laboratories, Via Enrico Fermi 40, I-00044 Frascati, Italy.
[4] INFN and Physics Department, University of Perugia, Via A. Pascoli, I-06123 Perugia, Italy

Received: date / Revised version: date

Abstract. In this paper we apply to photoproduction total cross-section a model we have proposed for purely hadronic processes and which is based on QCD mini-jets and soft gluon re-summation. We compare the predictions of our model with the HERA data as well as with other models. For cosmic rays, our model predicts substantially higher cross-sections at TeV energies than models based on factorization but lower than models based on mini-jets alone, without soft gluons. We discuss the origin of this difference.

PACS. PACS-key 13.60.Hb,13.85.Lg,12.40.Nn,12.38.Cy,11.80.Fv – PACS-key total and inclusive cross-sections,optical models,resummation,eikonal aproximation

1 Introduction

Cosmic ray experiments and planning for a future linear collider require knowledge of photon total cross-sections for values of very high c.m. energy of the photon-proton or photon-photon system, in regions where no data are available. In this paper we study the predictions of a mini-jet model, extending to the photon a model developed for proton-proton scattering [1]. We apply this model to photo-production, leaving to a later paper the application to photon-photon scattering.

Understanding the energy dependence of total hadro–nic cross-sections continues to be an important issue in the study of strong interactions per se [2]. Over the years, various descriptions of this energy dependence have been given. Some approaches have focused on how far one can reach following the basic principles of analyticity, unitarity, factorisation etc., without any recourse to the details of the particular hadron involved, whereas at the other end of the spectrum, there are models which include the fundamentals of QCD as far as possible and then try to compute the cross-section in terms of measured properties of the particular hadron. Of course, all descriptions have to be consistent with the requirements of analyticity and unitarity. Most descriptions involve a few "soft" (non-perturbative) parameters, which can not be determined through perturbative QCD. Again, basic symmetry, unitarity and factorisation arguments may at times lead to certain relationships among these soft parameters for various hadrons. Often they may be determined only through fits to the experimen-

tal data and then one may only test approximate relations among these indicated by general arguments. In short, understanding the behaviour of the total hadronic cross-section and other soft quantities such as multiplicities etc., from first principles, is an extremely challenging problem and as stated before, one has different answers with varying degrees of relationship to QCD.

Hadronic cross-sections for processes induced by the photon and the hadronic structure of the photon itself, have played a very interesting and important rôle, in furthering the attempts to understand the theoretical issues involved in the subject. Photon-hadron interactions offer the theorists one more laboratory to test their various ideas about computing "soft" quantities such as purely hadronic total cross-sections from basic principles. Historically, it is the interaction of the highly virtual photon with the hadron that offered the first glimpse of (almost free) quarks and later provided basic evidence for perturbative QCD being the correct dynamics to explain strong interactions in a certain kinematic domain. However, in the present context, it is the photon structure function language [3] used to describe interactions of the real or quasi–real photon (invariant mass square ~ 0), with other hadrons or photon, that is of interest. In fact, the structure function of a quasi real photon at large values of x_γ and that of a highly virtual photon (with large values of Q^2 where $-Q^2$ indicates the invariant mass square of the virtual photon) for all values of x_γ, can be computed using perturbative QED and QCD alone, for large values of momentum transfer square, Q^2 of the probe. However, equally important is the (non perturbative) part of the real (or quasi real) photon structure function at small x_γ which is not amenable to perturbative QCD (PQCD) computations.

In this paper, we apply our eikonal mini-jet model augmented by soft gluon resummation, which has been successful in providing an acceptable description of the $pp/p\bar{p}$ data, to the description of total cross-sections of photon induced processes. In our model for the (purely hadronic) proton total cross-sections, we were able to compute the relevant components in terms of basic QCD inputs such as the experimentally measured parton densities and QCD subprocess cross-sections along with a few non-perturbative parameters. Given the prior success, it becomes of interest to see how the predictions of our model, applied to the total hadronic cross-sections of photon induced processes and using the experimentally determined knowledge on the structure of the "real" photon, compare with the data. We shall be mainly concerned with the issue of its energy dependence.

To recapitulate: in this paper we explore the effects of the hadronic structure of the photon through studies of total cross-sections involving photons. While at low energy, these cross-sections can be obtained through factorization and vector meson dominance, the high energy range poses a different challenge. We have argued in a number of papers [3,4,5,6] that the energy dependence of the photon induced processes do not follow from a straightforward application of factorization properties of the total cross-sections. We shall discuss various factorization results [7, 8,9,10,11] and compare some of them with the HERA data [12,13] as well as with predictions of our QCD eikonal model with resummation, hereafter referred to as the BN model [14]. The reasons for this nomenclature will be clear as we describe the model. Some of its details are summarized in two Appendices, so as not to overburden the reader with material published elsewhere.

2 Total cross-sections: from pp to $\gamma\gamma$

Experimentally, all total cross-sections rise asymptotically with energy, but it is not yet clear whether the rate of increase is the same for different processes and whether their asymptotic behaviour is already controlled by the Froissart-Martin [15] bound. For any given total hadronic cross-section, this bound says that asymptotically

$$\sigma_{tot} \leq C(\log s)^2. \qquad (1)$$

From a theoretical point of view, this bound is only valid for the scattering of hadrons. Attempts to extend it to virtual photon process [16] have resulted in a less restrictive bound, but which cannot be extended to real photons,

leaving unanswered the question of whether the bound of Eq. (1) is valid also for real photons.

Phenomenologically, the LEP data [17] seem to indicate that the slope with which the total $\gamma\gamma$ cross-section rises is not the same as in the proton case[5]. This difference would spoil the simplicity of the so-called Regge-Pomeron model, in which the high energy rise is described through a single universal term [11]. Of course, all total cross-sections do rise and to appreciate it at a glance, we show in Fig. 1 a compilation of data on $pp/\bar{p}p$ [18][19], γp [12,13] and $\gamma\gamma$ [17] scattering together with expectations from the BN model [14] for protons to be described in the next section. Since the data span an energy range of four orders of magnitude, with the cross-sections in the millibarn range for proton-proton, microbarn range for photoproduction and nanobarns for photon-photon, to plot them all on the same scale, one needs a normalization factor. The data suggest to multiply the γp cross-section by a factor ≈ 330 and then $\gamma\gamma$ by $(330)^2$, as shown in Fig. 1.

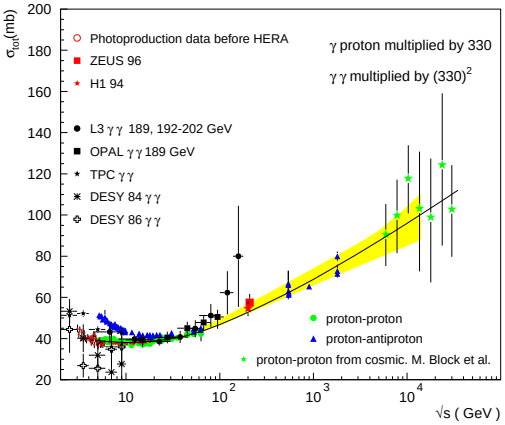

Fig. 1. Proton [19] and photon [12,13,17] normalized total cross-sections with the band expected from our BN model for $pp/\bar{p}p$ [1] and one typical curve from this model [14]. Cosmic ray data are from ref. [25].

It has been known for quite some time [20] that to get the photoproduction cross-section from the proton cross-sections in the region where they are approximately constant, namely after the initial Regge-exchange type fall and before the beginning of the high energy rise, the multiplicative factor to apply for each photon leg in the cross-section can be obtained from Vector Meson Dominance (VMD) (to go from a photon to a meson) and a quark counting factor, namely

$$R_\gamma = \frac{N_{meson}^{fermion\ lines}}{N_{proton}^{fermion\ lines}} P_{VMD} = \frac{2}{3}\Big(\sum_{V=\rho,\omega,\phi} P_V\Big) = \frac{2}{3}\Big(\sum_{V=\rho,\omega,\phi} \frac{4\pi\alpha}{f_V^2}\Big) \qquad (2)$$

With present ρ-meson data [21] and the relation

$$P_\rho = \frac{e^2}{f_\rho^2} = \frac{\alpha}{12}\frac{m_\rho}{\Gamma_\rho} \qquad (3)$$

we would obtain $R_\gamma \approx 1/360$, consistent with the value indicated in the figure.

Note that there is no a priori reason to expect the scaling factor to be energy independent. On the other hand, while at low energies the factor R_γ can be reliably evaluated through VMD, at high energies, it is likely to be different [22] due to the difference in the quark and gluon content of photons [3] versus that of the hadrons. The use of a simple multiplicative factor to compare the photon processes with each other and with the pure proton processes, is the simplest form of *factorization*. More complex forms of factorization exist in the literature, as in a recent formulation by Vereshkov and collaborators [23] or as in the model by Block et al. (also called the Aspen model) [24]. More comments shall follow in the last section.

The above discussion points to the need for a description of high energy photon interactions where reliable predictions can be made based on the quark-parton structure of the photon. As stated earlier, we have developed such a model for purely hadronic processes [1,14,26,27] which we shall extend and apply to photoproduction processes in the next section.

3 The Bloch-Nordsieck model (BN)

This model is based on the eikonal representation for the total cross-section [28,29], and the eikonal incorporates QCD inputs such as parton-parton cross-sections, parton densities extracted from perturbative QCD fits to the data, actual kinematics, and soft gluon resummation. In detail, we use:

1. QCD mini-jets [30,31] to drive the rise of the total cross-section in the QCD asymptotic freedom regime;
2. the eikonal representation for the total cross-section with the real part of the eikonal approximated to zero and the imaginary part obtained through mini-jet QCD cross-sections;
3. an impact parameter distribution obtained as the Fourier transform of the re-summed soft gluon transverse momentum distribution;
4. resummation of soft gluon emission down to zero momentum to soften the rise due to the increasing number of gluon-gluon collisions between low-x, but still hard perturbative, gluons.

While the eikonal representation with the mini-jet input has long been in use, our model differs from other existing eikonal models in that the impact parameter distribution is energy dependent and derived from soft gluon k_t-resummation, which gives the model its name.

Before turning to the application of the model to photon processes, we shall briefly discuss the various approximations involved.

1. the energy dependence of QCD mini-jets reflects the increase -at low x- of the gluon structure functions and this can provide a mechanism for the rise of total cross-sections. However, parton-parton cross-sections require a minimum transverse momentum cut-off to avoid the $1/p_t^2$ divergence. Fixing such a cut-off around 1 GeV, leads to an extremely sharp rise. Our model starts with this input and then tempers the rise through the energy-dependent impact parameter distribution.
2. the eikonal representation for total cross-sections is an approximation which allows one to enforce the requirement of s-channel unitarity. Here one obtains the total cross-sections through the eikonal formulae

$$\sigma_{tot} = 2 \int d^2\boldsymbol{b}[1 - e^{-\Im m\chi(b,s)} \cos \Re e\chi] \quad (4)$$

$$\sigma_{el} = \int d^2\boldsymbol{b}|1 - e^{i\chi(b,s)}|^2 \quad (5)$$

$$\sigma_{inel} = \int d^2\boldsymbol{b}[1 - e^{-2\Im m\chi(b,s)}] \quad (6)$$

The introduction of the jet cross-section as the term which drives the rise in the eikonal function can be done unambiguously through the inelastic cross-section, which only depends upon the imaginary part of the eikonal function. Notice that the expression for σ_{inel} can also be obtained upon summing multiple collisions which are Poisson distributed with an average number $n(b,s) = 2\ \Im m\ \chi(b,s)$. Using the experimental value of the ρ parameter (the ratio of the real to the imaginary part of the forward elastic amplitude) for pp and $p\bar{p}$ processes, we can estimate only about 4% correction from the real part. Hence, we assume $\Re e\chi = 0$, and thus obtain a very simple approximate expression

$$\sigma_{tot} = 2 \int d^2\boldsymbol{b}[1 - e^{-n(b,s)/2}] \quad (7)$$

which can be used to test our ideas about the underlying strong interaction dynamics.
3. the impact parameter distribution, which contains all the b-dependence, represents the matter distribution in the colliding hadrons and our model obtains it as the shadow of the path followed by the partons as they scatter through the hadronic matter. The scattering process defines the partonic densities in the transverse plane.
4. soft gluon emission is a QCD mechanism which introduces acollinearity and thus can reduce the LO parton-parton cross-section. We use the resummation scheme obtained first in QED by Yennie, Frautschi and Suura [32], extended to QCD transverse momentum (k_t) distributions in refs. [33,34], applied to Drell-Yan pair and W-production in [35,36], as well as to jet production in [37]. Earlier, we had discussed such k_t-resummation scheme for con-

stant but large values of the coupling constant in [38]. As we discuss in Sect. 4, this resummation scheme includes an integration over the zero momentum modes. Depending on the (yet unknown) behaviour of α_s in this region, the integral over the low energy part of the single soft gluon distribution may become relevant. Similar integrals, involving α_s in the infrared region have been discussed in [39] as being related indeed to physical observables. For the transverse momentum case, this integral is usually absorbed in the intrinsic transverse momentum of the scattering hadrons and considered to be a constant. Our approach differs and has been discussed in [1] and references therein. We shall return to this in Sect. 4.

The BN model was applied to proton-proton scattering, obtaining a total cross-section at LHC $\sigma(\sqrt{s} = 14\ TeV) = 100 \pm 12\ mb$, where the error reflects various uncertainties such as in the choice of parton densities for the proton, minimum parton p_t cut-off, called p_{tmin}, and the infrared behaviour of soft gluon coupling. Thus, the model has a number of parameters, some of which have a physical meaning associated with confinement. As such, we do not know how and if to change them as one goes from protons to photons. We shall try to vary them by no more than (5-10)% from their values for the proton. Whenever a stronger variation is required, we shall comment upon it. The model predictions are obviously dependent on the parton densities in the photon: as in the case of the proton, we have employed different available sets, obtained by fits to the data on the photon structure function F_2^γ, and seen how best to describe the available data without appreciably changing the parameters. Application to photons however requires an additional insight. In the eikonal representation we need to *adapt* the hadronic language to that for the photon. One first needs the probability, P_{had}, that a photon behaves like a hadron and subsequently one may then use the eikonal representation, as in Refs. [24, 40, 41]:

$$\sigma_{tot}^{\gamma p} = 2P_{had} \int d^2\boldsymbol{b}[1 - e^{-n^{\gamma p}(b,s)/2}]. \quad (8)$$

Eq. 8 has no *ab initio* derivation. It is an approximation, used in minijet inspired descriptions of photon cross-sections, useful to model the low energy term and provide a normalization for the cross-section. One could expect P_{had} to have an energy dependence or b-dependence, or both. However, to compare our model with other mini-jet models in the literature, and to make the simplest possible extension of our model from protons to photons, we consider it to be a constant as far as energy is concerned. As for the impact parameter space and related energy dependence, these effects are obtained in our model through QCD soft gluon resummation, just as in the case of protons.

In Eq. 8 the real part of the eikonal has been approximated to zero, again following the proton model, while the imaginary part is obtained from the average number of inelastic collisions for a given impact parameter b, $n^{\gamma p}(b, s)$, at a given c.m. energy $\sqrt{s}$. Following our BN model for protons, we distinguish between collisions calculable as QCD mini-jets, and everything else, writing the average number of collisions as

$$\begin{aligned} n^{\gamma p}(b, s) &= n_{soft}^{\gamma p}(b, s) + n_{hard}^{\gamma p}(b, s) \\ &= n_{soft}^{\gamma p}(b, s) + A^{\gamma p}(b, s)\sigma_{jet}^{\gamma p}(s)/P_{had} \end{aligned} \quad (9)$$

with n_{hard} including all outgoing parton processes with $p_t > p_{tmin}$. In Eq. 9 the impact parameter dependence has been factored out, averaging over densities in a manner similar to what was done for the case of the proton in [27]. Because the jet cross-sections are calculated using actual photon densities, which themselves give the probability of finding a given quark or gluon in a photon, P_{had} needs to be canceled out in n_{hard}. As for its value, $P_{had} \approx P_{VMD}$. P_{had} is *not* the same numerical factor R_γ used in Fig. 1 to normalize all the cross-sections at low energy, but it can be connected to it by making an expansion of the eikonal in the low energy region, where $\sigma_{jet} \approx 0$, as shown at the end of this section. Also, while P_{had} can be factored out in some models, as we shall see later, this does not happen in the BN model.

The mini-jet cross-section is obtained by integrating the standard QCD inclusive jet cross-section, using a lower cutoff p_{tmin} as described

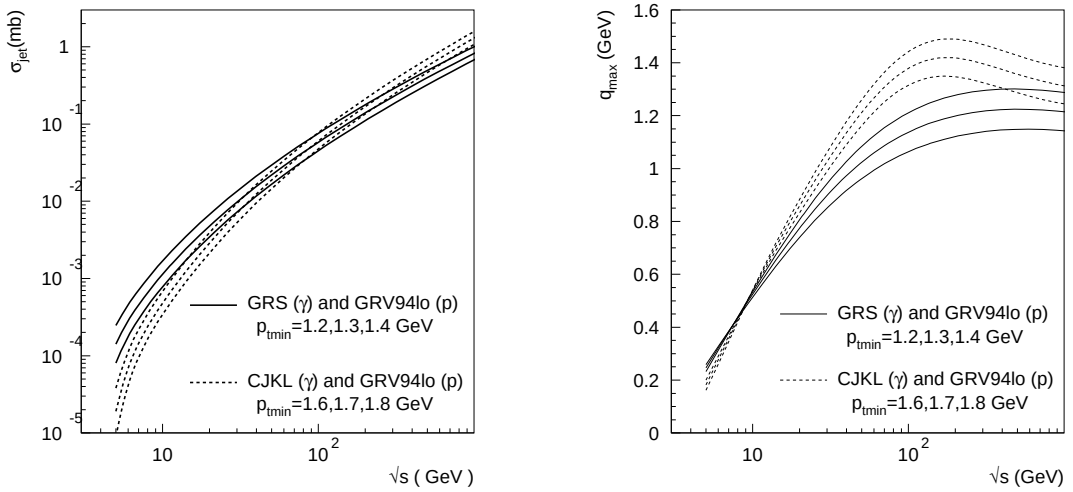

Fig. 2. Left panel: Photon-proton jet cross-sections for different densities and a range of p_{tmin} values. Right panel: average value of the maximum transverse momentum allowed for single initial state soft gluon emission, in γp scattering.

in Appendix A. The mini-jet cross-sections are to be calculated using parton densities (PDFs) for the proton and photon determined from perturbative QCD analysis of the data on F_2^p, F_2^γ as well as a variety of other data on hard processes for the proton. Common ones for the proton are GRV [42], MRST [43], CTEQ [44], whereas those for the photon are GRV[45], GRS [46], CJKL [47]. These densities are available both at leading order (LO) or higher, but in our model we use only the LO ones, as part of the NLO effects are described by soft gluon resummation and the use of NLO would result in some double counting. Of course, in using densities and parton-parton cross-sections only at LO but with resummation of soft gluons, our model lacks the non-infrared part of the NLO corrections. Since we consider the resummation effects in the infrared region to be the most important for saturation and these are easily incorporated in our model, we have opted for LO densities, and thus also tree level parton-parton cross-sections and one loop α_s. We show in Figure 2 the energy dependence of the mini-jet cross-sections for γp collisions, for two different sets of parton densities for the photon, GRS and CJKL. We have used different values of the cut-off, namely $p_{tmin} = 1.2, 1.3, 1.4\ GeV$ for GRS densities, higher values for the case of CJKL densities, which give jet cross-sections rising faster with energy than those calculated using GRS [48]. As for the proton densities, we have done all the model calculations using GRV94.

These cross-sections grow very rapidly with energy, reflecting the infinite range of QCD. Since the finiteness of strong interactions is reflected by the finite spatial extension of hadrons, one expects that the eikonal representation would check such growth through the impact parameter distribution which appears in Eq. 8. A frequently used distribution is obtained as a convolution of the form factors of the colliding hadrons [49], namely

$$A_{FF}^{AB}(b) = \int \frac{d^2\boldsymbol{q}}{(2\pi)^2} \mathcal{F}^A(q)\mathcal{F}^B(q) e^{i\boldsymbol{q}\cdot\boldsymbol{b}}. \qquad (10)$$

However, it was noted already in case of proton cross-section [26] , that, without the inclusion of additional parameters, this choice is unable to reproduce both the early rise and the expected, Froissart -like, subsequent leveling off at high

energies. Apart from this purely phenomenological consideration, the form factor description becomes undefined when dealing with photons. For photons, such models, labeled as Form Factor (FF) models, depend on how one defines the photon form factor. In the literature, early attempts to apply the mini-jet eikonalized expression to the photon cross-sections [40] used a monopole expression for the photon (as in the pion case) and the usual dipole expression for the proton form factor with $\nu^2 = 0.71\ GeV^2$, obtaining

$$A^{\gamma p}_{FF} = \frac{1}{4\pi}\frac{\nu^2 k_0^2}{k_0^2-\nu^2}[\nu b \mathcal{K}_1(\nu b) - \frac{2\nu^2}{k_0^2-\nu^2}(\mathcal{K}_0(\nu b) - \mathcal{K}_0(k_0 b))] \quad (11)$$

with $k_0^2 = 0.44\ GeV^2$. The above expression can be adapted to photon data by varying the parameter k_0, and then the pion form factor expression for the photon can be understood to represent an intrinsic transverse momentum [50, 51]. In the Aspen model [24] another possibility has been explored. Namely, the overlap function is parametrized as the Fourier transform of a dipole form factor

$$W(b,\mu) = \frac{\mu^2}{96\pi}(\mu b)^3 K_3(\mu b) \quad (12)$$

with three different scaling parameters for the three terms in which the eikonal is split, quark-quark, quark-gluon or gluon-gluon scattering. In this model, one then uses a single functional expression for the b-distributions in hadron-hadron, hadron-photon or photon-photon scattering, but the difference between these different processes is provided through the μ parameters which scale among the various processes according to the additive quark model. In another QCD inspired model[52], a similar modelling has been made.

More fundamental attempts to obtain the photon impact factor in the context of perturbative QCD can be found in [53] and references therein. However, since these models are derived for virtual photon scattering, they cannot be used in the context of our BN mini-jet model, which is applied to real photon processes, with real photon parton densities. In this paper we follow the same strategy which we used in case of the proton cross-sections and, for hard collisions, use mini-jets and soft gluon resummation, with n_{hard} given by:

$$n^{\gamma p}_{hard}(b,s) = \frac{A^{\gamma p}_{BN}(b,s)\sigma^{\gamma p}_{jet}}{P_{had}} \quad (13)$$

with

$$A^{\gamma p}_{BN}(b,s) = \mathcal{N}\int d^2\mathbf{K}_\perp \frac{d^2P(\mathbf{K}_\perp)}{d^2\mathbf{K}_\perp} e^{-i\mathbf{K}_\perp\cdot\mathbf{b}} = \frac{e^{-h(b,q_{max})}}{\int d^2\mathbf{b} e^{-h(b,q_{max})}} \equiv A_{BN}(b,q_{max}(s)). \quad (14)$$

The function $A^{\gamma p}_{BN}$ is normalized to 1 and is obtained from the Fourier transform of the soft gluon resummed transverse momentum distribution, whose structure we discuss in the next section.

To complete the calculation of $n^{\gamma p}_{hard}$, one has to specify the value of P_{had}, which in eikonal models [24,41] indicates the probability that a photon behaves like a hadron and is defined by the low energy part of the cross-section. At low energy, namely for $\sqrt{s} \approx 5 \div 10\ GeV$, the mini-jet cross-section is very small and $n(b,s)^{\gamma p} \approx n^{\gamma p}_{soft}(b,s)$. This part of the cross-section is outside the range of perturbative QCD we have described so far. Using Eq. 8, we find that we can get a good description of the low energy γp data for the total cross-section with

$$n^{\gamma p}_{soft}(b,s) = \frac{2}{3} n^{pp}_{soft}(b,s) \quad (15)$$

where $n^{pp}_{soft}(b,s)$ is the same function we have used for our description of proton-proton collision in ref. [1] and $P_{had} = 1/240$, a result consistent with Eq. 2.

4 The impact parameter distribution and the saturation parameters

The distribution A_{BN} is energy dependent through the quantity $q_{max}(s)$, which represents the average maximum transverse momentum allowed to a single soft gluon emitted in the initial state in a given hadronic collision. This quantity is the

input to the kernel $h(b, q_{max})$, which describes the exponentiated, infrared safe, number of single soft gluons of all allowed momenta and is given by,

$$h(b, q_{max}(s)) = \frac{16}{3}\int_0^{q_{max}(s)} \frac{dk_t}{k_t}\frac{\alpha_s(k_t^2)}{\pi} \times \left(\log\frac{2q_{\max}(s)}{k_t}\right)[1 - J_0(k_t b)] \quad (16)$$

In the BN model, this function provides the cut-off in impact parameter space which softens the rapid rise of the mini-jet cross-section. To render this point clear, we shall summarize and outline our argument in what follows.

The soft gluon resummation formula in the transverse momentum variable has been known for a long time and reads [33,34,38]:

$$d^2P(\mathbf{K}_\perp) = d^2\mathbf{K}_\perp \int \frac{d^2\mathbf{b}}{(2\pi)^2} e^{-i\mathbf{K}_\perp\cdot\mathbf{b} - h(b,q_{max}(s))} \quad (17)$$

with

$$h(b, q_{max}(s)) = \int_0^{q_{max}(s)} d^3\bar{n}(k)[1 - e^{i\mathbf{k_t}\cdot\mathbf{b}}] \quad (18)$$

where $q_{max}(s)$ is the maximum transverse momentum kinematically allowed for single emission. The expression in Eq. 17 can be obtained from the more general expression for soft resummation

$$d^4P(K) = d^4K \int \frac{d^4x}{(2\pi)^4} e^{iK\cdot x - h(x,E)} \quad (19)$$

with $h(x, E)$ similarly defined as in Eq. 18. This expression was obtained long time ago in QED [32], with order by order cancellation of the infrared divergence in perturbation theory. Notice that the same expression is obtained very simply in a semi-classical way using the methods of statistical mechanics and imposing energy momentum conservation [54]. In such derivation, it is energy-momentum conservation that brings in the cancellation of the infrared divergence between soft and real quanta emission.

In QED, $d^3\bar{n}(k) \propto \alpha\log(\frac{2q_{max}}{m_{electron}})$ and resummation in the transverse momentum variable is well approximated by a first order expansion in α. For large values of the coupling constant however, this approximation would be inadequate and we noticed long time ago [38] that, for such cases, resummation of soft quanta emission can provide a transverse momentum cutoff, based on the expansion of the Bessel function $J_0(k_t b)$ around $k_t b \approx 0$.

In QCD [33,34], Eq. 18 shows the presence of a non-trivial complication, namely the impossibility to use the asymptotic freedom expression for α_s down to $k_t = 0$. It is this non-trivial complication which we exploit to study scattering in the very large impact parameter region.

To overcome the difficulty arising from the infrared region, the function $h(b, E)$, which describes the relative transverse momentum distribution induced by soft gluon emission from a pair of, initially collinear, colliding partons at LO, is split into

$$h(b, E) = c_0(\mu, b, E) + \Delta h(b, E), \quad (20)$$

where

$$\Delta h(b, E) = \frac{16}{3}\int_\mu^E \frac{\alpha_s(k_t)}{\pi}[1 - J_o(bk_t)]\frac{dk_t}{k_t}\ln\frac{2E}{k_t}. \quad (21)$$

Since, in $\Delta h(b, E)$, the integration only extends down to the scale μ (not zero), the $J_o(bk_t)$ is assumed to oscillate to zero and hence is dropped. The last integral is now independent of b and can be performed, giving

$$\Delta h(b, E) = \frac{32}{33 - 2N_f} \left\{\ln(\frac{2E}{\Lambda})\left[\ln(\ln(\frac{E}{\Lambda})) - \ln(\ln(\frac{\mu}{\Lambda}))\right] - \ln(\frac{E}{\mu})\right\}. \quad (22)$$

where Λ being the scale in the asymptotic freedom expression for α_s. In the range $1/E < b < 1/\Lambda$ the effective $h_{eff}(b, E)$ is obtained by setting $\mu = 1/b$ [34]. This choice of the scale introduces a cut-off in impact parameter space which is stronger than any power, since the radiation function is now

$$e^{-h_{eff}(b,E)} = [\frac{ln(1/b^2\Lambda^2)}{ln(E^2/\Lambda^2)}]^{(16/25)ln(E^2/\Lambda^2)} \quad (23)$$

which is Equation(3.6) of ref. [34]. The remaining b-dependent terms in $h(b, E)$ are dropped, a reasonable approximation if one assumes that there is no physical singularity in the range of integration $0 \leq k_t \leq 1/b$. However, when the integration in impact parameter space extends to very large b-values, as is the case for the calculation of total cross-sections, this expression fails to reproduce the entire range of the energy dependence of low energy transverse momentum effects. To explore the very large b-region, we suggest to use Eq. (16) with its full integration range, proposing a phenomenological approach to the zero-momentum soft gluons [55]. Our approach uses a singular, but integrable expression for α_s: this allows us to extend the integral to the minimum allowed value zero and to obtain a b-dependence which is stronger than the one of Eq. 23.

Thus the infrared region can provide an impact parameter cutoff at large b-values, provided the integral is finite. This requires any proposed expression for α_s in the infrared region to be integrable. As discussed in detail in ref. [26], the actual functional dependence of the cut-off depends on the model for α_s in the infrared. Here we mention that in the model we propose, the resulting cut off in b-space is at least an exponential function.

In the next subsections, we shall discuss various proposals to model the infrared region and how the full integral of Eq. (16) controls the saturation of the cross-section through its limits of integration. We shall see that our model for soft gluon emission is regulated by a constant infrared parameter p and the energy dependent momentum function q_{max} as follows:

1. the energy dependent momentum saturation parameter $q_{max}(s)$ depends on the energy behaviour of the density functions of colliding partons and on p_{tmin}, the mini-jet cut-off,
2. the infrared parameter p, to be specified shortly, defines the infrared behaviour of $\alpha_s(k_t^2)$. The closer its value is to 1, the more the mini-jet cross-sections will be quenched at any given energy.

4.1 The momentum saturation parameter $q_{max}(s)$

For any given parton parton collision, $q_{max}(s)$ can be defined by kinematics. We introduced this quantity for the first time in [27] to represent the maximum transverse momentum carried by a single gluon, averaged over the basic scattering cross-section with a procedure described in Appendix B for the convenience of the reader. To highlight the physical meaning of $q_{max}(s)$, let us define the saturation parameter

$$\hat{\kappa} = \frac{\sqrt{\hat{s}} - \sqrt{\hat{s}_{jets}}}{\sqrt{\hat{s}}/2} \tag{24}$$

for each parton pair of c.m. sub energy $\hat{s}$ which scatters into a final parton pair of c.m. energy $\sqrt{\hat{s}_{jets}}$. Let us now use the kinematics of the process

$$parton(x_1)+parton(x_2) \rightarrow gluon(k_t)+jet_1+jet_2 \tag{25}$$

to write the maximum transverse momentum of the emitted gluon, in the case of limited energy loss as [56]

$$k_{tmax} = \frac{\sqrt{\hat{s}}}{2}(1 - \frac{\hat{s}_{jets}}{\hat{s}}) \approx \frac{\sqrt{\hat{s}}}{2}\hat{\kappa} \tag{26}$$

This quantity plays an important role in our model. As the available c.m. energy increases, it increases, depending upon the probability of producing a parton pair scattering into a given final state. It thus depends upon the densities and the parton-parton cross-section. As it increases, more and more acollinearity is introduced in the scattering and the stronger is then the reduction in the growth of the mini-jet cross-section.

Notice that now there appear two different scales and both low-x perturbative gluons as well as soft gluons. We stress the distinction between them: low-x gluons participate in the hard parton-parton scattering described by the mini-jet cross-section discussed in the previous section, for which

$$p_{tout} \equiv p_t^{jet} \geq p_{tmin} \approx 1 \div 2 \ GeV \tag{27}$$

These low-x perturbative gluons interact with a strength proportional to $\alpha_s(p_{tout}^2)$, while soft

gluons are those emitted, from the initial state, in any given parton-parton process with transverse momentum

$$k_t \leq k_{tmax} \approx 10 \div 20\% \; p_{tout} \qquad (28)$$

This scale, k_{tmax} defines the single soft gluons, whose number can be indefinite. These soft gluons need to be re-summed through the procedure which results in the exponentiated factor of Eq. 14.

In a model such as ours, which is not a Monte Carlo simulation of the processes involved, we have opted for averaging these effects, embodying them in a factorized expression such as that given by Eq. 14, with k_{tmax} averaged out to obtain q_{max}, as shown in Appendix B. The expression for $q_{max}(s)$ depends both on the parton densities and the value of p_{tmin}. The resulting quantity is energy dependent since the densities are energy dependent through the applied DGLAP evolution. The averaging process done in this model includes only quark densities as the source of the leading acollinearity effect. We consider the leading effect to arise because of soft gluon emission from the external legs of the scattering process, valence quarks for the proton beam and all flavours of quarks for the photons. An improvement of the model could include soft gluon emission also from the low-x perturbative gluons, as we shall discuss in a forthcoming paper. In the right-hand panel of Fig. 2 we show the dependence of $q_{max}(s)$ upon the c.m. energy of the colliding particles, for the same densities and p_{tmin} values used in the mini-jet cross-sections shown in the left panel.

As q_{max} increases with energy, the growth of the total cross-section due to mini jets is tempered by soft gluon emission, through the exponential damping factor $e^{-h(b,q_{max})}$. However, there is an equilibrium between the increase of q_{max} and the rate of increase of the mini-jet cross-section since one reflects the quarks and the other the gluon densities. The distribution of these partons at high energy follows the parton sum rules and one is not independent of the other. From the right hand panel of Fig. 2 we see that q_{max}, for both GRS and CJKL densities, will reach some sort of saturation at high energies, which reflects in the total cross-sections reaching a stable slope.

The momentum saturation parameter q_{max} is not the only quantity which gives rise to saturation, the infrared limit of α_s also plays a major role. We shall discuss this in the next subsection.

4.2 A phenomenological approach to the infrared limit of α_s

To complete the calculation of the impact parameter distribution for hard processes in γp collisions, we need to discuss the lower limit of integration in Eq.16. Usually, the soft gluon resummation formula extends the soft gluon momenta to an infrared cut-off taken to correspond to the intrinsic transverse momentum scale of the scattering hadrons [33,34]. Instead, in our model, we extend the integration down to the zero momentum modes.

The reason to do so lies in the nature of the cancellation of the infrared divergence. To obtain this cancellation, it is mandatory that virtual and real soft gluon emission join in the zero momentum limit. Of course we do not know how to deal with α_s in this limit and for this reason the integral over this region is usually left out and substituted with a constant intrinsic transverse momentum. However, this part of the integral is relevant for many minimum bias processes, as pointed out in ref. [39]. With our model, we aim to relate the behaviour of the impact factor at very large b-values with the infrared region of soft gluon emission.

To do so, we need therefore to make an ansätz as to the behaviour of the strong coupling constant in the infrared region, where the usual asymptotic freedom expression for $\alpha_s(Q^2)$ cannot be used. One possibility is to use an expression which would go to a constant as $Q^2 \to 0$ as in

$$\alpha_s(Q^2) = \frac{12\pi}{33 - 2N_f} \frac{1}{\log[a + \frac{Q^2}{\Lambda^2}]} \qquad (29)$$

with $a \approx 2$ [57,35] and $\Lambda = \Lambda_{QCD}$. This expression is often referred to as the *frozen* α_s case. Another possibility is to employ the Richardson potential for quarkonium, which uses a singular

α_s, namely $a = 1$, so that

$$\alpha_s^R(Q^2) \approx \frac{1}{Q^2} \qquad Q^2 \to 0 \qquad (30)$$

The Richardson potential has been shown to give good results to describe charmonium states [58], but it cannot be used here because the integral over the soft gluon modes would diverge. The reason it works in quarkonium applications is that in that case one never actually reaches values corresponding to $Q^2 = 0$, since the potential binds the two quarks in a region of space at fixed finite distance of $\mathcal{O}(r_{Bohr})$.

In order to be able to use the Richardson-like α_s^R, we soften the singularity with the proposal that in the infrared limit, one can phenomenologically use the expression

$$\alpha_s(k_t) = constant \times \left(\frac{\Lambda}{k_t}\right)^{2p} \qquad k_t \to 0 \quad (31)$$

where Λ is a cut-off of order Λ_{QCD}, and p is a parameter which embodies the infrared behavior, with $p < 1$ so that the soft gluon integrals converge. For the time being, we consider the above expression as a phenomenological ansätz . The constant in front of Eq. 31 should be chosen to provide a smooth extrapolation to the perturbative expression for α_s. Our choice for the interpolating function is

$$\alpha_s = \frac{12\pi}{33 - 2N_f} \frac{p}{\ln[1 + p(\frac{k_t}{\Lambda})^{2p}]} \qquad (32)$$

This expression was also introduced to describe the intrinsic transverse momentum of Drell-Yan pairs, with the choice $\Lambda = 100\ MeV$ [55] and $p = 5/6$. This choice for the infrared behaviour (zero momentum gluons) was motivated [14] by an argument due to Polyakov [59]. It is clear that the closer p is to 1, the bigger the soft gluon integral $h(b, q_{max}(s))$ is and the stronger the saturation effects will be.

We shall show the results for the total γp cross section for this and other models in the next section.

5 Total γp cross-section at accelerator energies

In this section we examine the data on $\sigma_{\gamma p}^{\rm tot}$, starting from the low energy photoproduction data [18] up to the high energy HERA data and compare them with model predictions. In fact, HERA studied *ep* scattering and not only yielded information on energy dependence of the photoproduction cross-sections but also on $\gamma^* p$ cross-sections for different values of virtuality (invariant mass $-Q^2$) of the photon. For small values of x_γ and Q^2, the measurement of $F_2(W^2, Q^2)/Q^2$, where W is the invariant mass of the $\gamma^* p$ system, gives a measurement of $\sigma^{\gamma^* p}$ through the relation,

$$\sigma^{\gamma^* p} \simeq \frac{4\pi^2\alpha}{Q^2} F_2(W^2, Q^2)$$

The extrapolation of the measured quantity on the right hand side can then give the photoproduction cross-section in the limit $Q_\gamma^2 = 0$ [60]. The extrapolation of data collected with the ZEUS Beam Pipe Calorimeter (BPC) [61], based on a Generalized Vector Meson Dominance model, produces [62,63] a set of measurements in a continuous energy range $W_{\gamma p} = 104 \div 251\ GeV$ consistent within errors with the photoproduction data. The systematic errors are due to the GVMD extrapolation, with the longitudinal cross-section $\sigma_L = 0$, of the ZEUS BPC95 data. In the comparison, we have also included some cosmic ray data [64] which are in an energy range lower than HERA data, but higher than the older photoproduction data.

Let us start with the BN model for photons as described in the previous section. We have used GRV densities for the protons [42] and have varied the photon densities, using both GRS and CJKL. We show the result of the model and the dependence upon the model parameters in Figs. 3,4. In Fig.3 we have varied p_{tmin} and the densities to describe the high energy data from HERA in addition to the most acceptable description of the beginning of the rise, while keeping the parameter p in a range close to the $pp/\bar{p}p$ case. In Fig. 4 we have allowed for a larger variation in the value of the infrared parameter p, fixing the

PDF set and a range of appropriate values for p_{tmin}.

In order to obtain a good model description, we shall focus not only on the HERA data, but also on the beginning of the rise, as this signals the onset of the contribution of QCD processes and is strongly dependent upon p_{tmin}. We can see from Fig. 2 that, for the range of p_{tmin} values of interest, the mini-jet cross-sections calculated with CJKL densities rise faster than those calculated with GRS. It follows that, to describe the same HERA data, one will need to use different values of p_{tmin} depending upon the PDF set used. Thus CJKL densities call for a larger p_{tmin} than GRS densities. In Fig. 3 the infrared parameter p has been kept close to the value determined from the $pp/\bar{p}p$ cross-section, namely $p \approx 0.7 \div 0.8$. We see that the range of acceptable p_{tmin} values for GRS densities is not far from those used in the $pp/\bar{p}p$ case, where $p_{tmin} \approx 1.1 \div 1.25\ GeV$, but it is higher for CJKL.

To summarize the results of these figures, the latest HERA data are well described for a range of parameters $p = 0.75 \div 0.8$ and $p_{tmin} = 1.2 \div 1.3\ GeV$, to be compared with the pp and $\bar{p}p$ case where the range was very similar, with our central value $p = 0.75$ and $p_{tmin} = 1.15\ GeV$ for GRV densities. A good description is also obtained with CJKL densities, but then one needs a different $\{p, p_{tmin}\}$ set, as one reads from the second panel in Fig. 3.

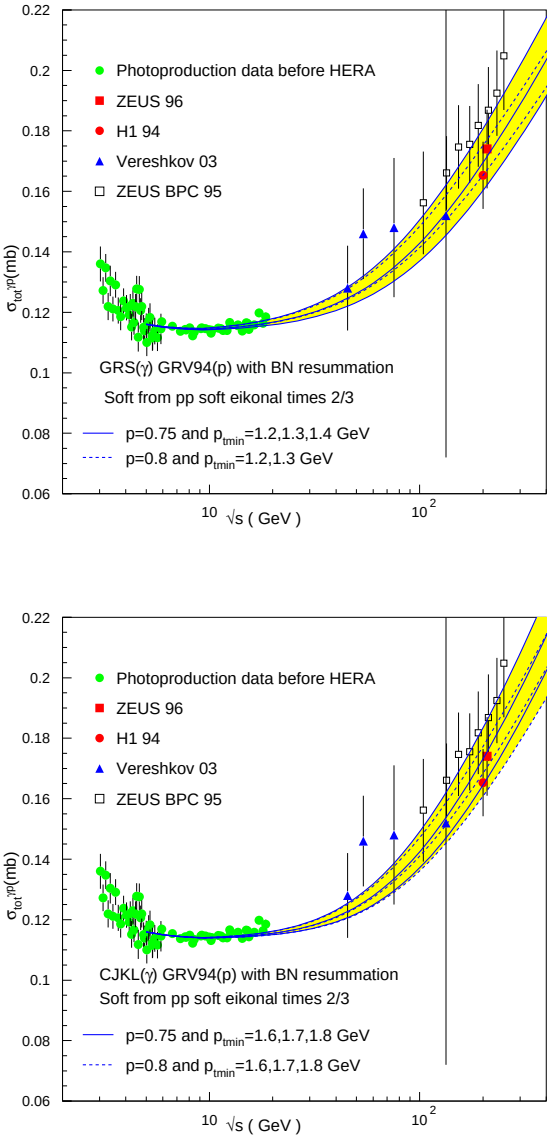

Fig. 3. Total γp cross-section with a range of parameter values close to the proton case, GRV densities for the proton and GRS or CJKL densities for the photon. Data from HERA are from Zeus [13], H1 [12] and a set of data from the ZEUS BPC extrapolated from $Q^2 \neq 0$ [60,62,63].

5.1 Parameter dependence

In the previous figures, we have applied the BN model for protons to γp scattering. No attempt has been made to choose one particular curve through an evaluation of the χ^2 of our curves with respect to the data. This is so because the aim of this paper is to extend the BN model to photon processes with as little changes as possible from the proton case. Another reason is that the data have rather large errors, and are extracted from very different experimental situations, which range from cosmic rays to HERA data on photoproduction to extrapolations of data collected with the ZEUS BPC. We did not wish to select one particular data set and adopted the

strategy to see whether the range of parameter values used for the proton results give curves consistent with the photo-production data.

The high energy behaviour of the model depends on the following entries:

1. PDF set, for which we have used GRV for the proton and GRS or CJKL for the photon
2. minimum hard parton cutoff p_{tmin}
3. infrared parameter p

with the choice of p_{tmin} related to the chosen PDF set. Of the two parameters, p_{tmin} is basically fixed so as to reproduce the early rise, where soft gluon resummation is not yet important, while the parameter p controls the quenching of the rise at high energy and also the absolute value of $n_{hard}(b,s)$. We also use $p_{tmin} \approx 1 \div 2\ GeV$ for the perturbative mini-jet calculation to make sense. The dependence on densities and p_{tmin} was shown in Fig. 3, while the parameter p was kept within the range of values used for the proton case. We see that the GRV/GRS density set is the one for which the extrapolation of the model from protons to photons works better. On the other hand, the model is also able to describe the data using CJKL densities, but in such case, the parameters are different from the proton scattering case. In Fig. 4 we give examples of how it is possible to quench the high energy rise from a given choice of PDFs (CJKL, in this example) through the parameter p. Notice that to catch the early rise, around $\sqrt{s} = 20\ GeV$, for CJKL densities one needs $p_{tmin} \approx 1.5\ GeV$, but then this requires a larger p-value in order to quench the rise and not overshoot the HERA data points.

All in all, we can say that the model adequately describes the photon-proton cross-section data and we can try to extend it to higher energies so as to make predictions for cosmic ray energies to be reached by the AUGER experiment [65,66]. We turn to this problem in the next section. But before this, we address the question of factorization: is a photon like a proton just multiplied by a constant factor? From what we have seen so far, one could describe γp total cross-section up to HERA energies either through a microscopic model such as our BN model, with quarks and gluons, or through other approaches

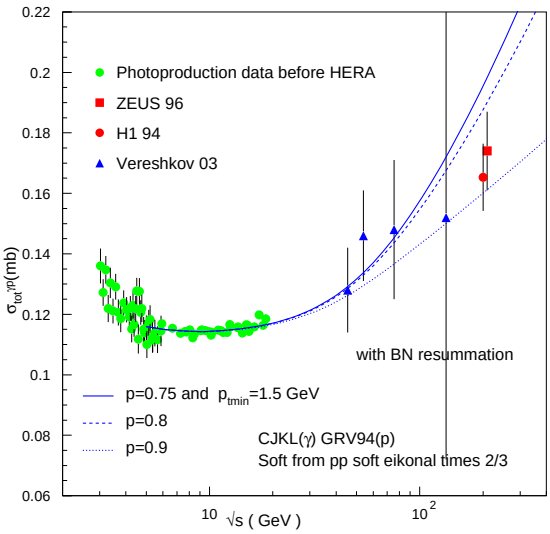

Fig. 4. Total γp cross-section with GRV for proton and CJKL densities for the photon, for a spread of p values.

based on various forms of factorization. In particular, the Aspen model also gives a good description as do other approaches, based on multiplying the result of fitting $pp/\bar{p}p$ data with a constant factor. We shall discuss this point in the coming subsection.

5.2 Factorization: a hadron-like photon

In the previous section, we have applied our model to the total γp cross-section, using available photon densities, going through the various steps defining our model, namely calculation of mini-jet cross-sections, evaluation of the energy dependence saturation parameters, determination of the energy dependent impact parameter function from soft gluon resummation $A_{BN}(b, q_{max}(s))$ and finally eikonalization. In this approach, at high energy, the photon is an independent entity from a hadron, with the rising behaviour of the cross-section and the b-distribution of the γp collision determined independently from other $hadron - hadron$ collisions such as pp. This is

different from other models, for instance the Aspen model [24], where the photon properties are obtained through scaling factors inspired by the additive quark model. As a consequence, in the Aspen model for photons, one can prove a factorization property [8] which would then allow to extract the $\gamma\gamma$ cross-section simply as [7]

$$\sigma_{tot}^{\gamma\gamma} = \frac{(\sigma_{tot}^{\gamma n})^2}{\sigma_{tot}^{nn}} \tag{33}$$

with σ_n to indicate the nucleon cross-sections. We shall discuss the $\gamma\gamma$ cross-sections within our BN model for photons in a separate paper, however we notice that such factorization is not to be expected in the model we present here.

Other types of factorization models are based on the Regge-Pomeron exchange, keeping a constant universal behaviour of the rising part of the cross-section with coefficients based on the factorization of the residues at the poles in the elastic amplitude, so that

$$\sigma_{tot}^{nn} = X_{nn}s^{-\eta} + Y_{nn}s^{\epsilon} \tag{34}$$

$$\sigma_{tot}^{\gamma n} = X_{\gamma n}s^{-\eta} + Y_{\gamma n}s^{\epsilon} \tag{35}$$

$$\sigma_{tot}^{\gamma\gamma} = \frac{(X_{\gamma n})^2}{X_{nn}}s^{-\eta} + \frac{(Y_{\gamma n})^2}{Y_{nn}}s^{\epsilon} \tag{36}$$

with $\epsilon \approx 0.08 \div 0.09$. This type of factorization is of course different from the one in Eq.33, but it still implies the idea that there is a universal behaviour of the energy dependence, not only at low energy, where one can confidently assume that the hadronic interactions of the photons are those of a vector meson, but also at high energy.

Such a description of the photon, i.e, that the photon is always hadron-like, could be reflected in our model by simply scaling the BN cross-section for protons, as

$$\sigma_{tot}^{\gamma p} = R_\gamma \sigma_{tot}^{pp} = R_\gamma \; 2\int d^2\boldsymbol{b}[1 - e^{-n^{pp}(b,s)/2}] \tag{37}$$

Present accelerator data for γp are consistent with factorization models, including an application as given in Eq. 37, but as we shall see in the next section, at higher energies, expectations will differ.

6 Extrapolation to very high energies

In this section we extend our calculation beyond present accelerator energies and compare our predictions with other approaches. We start with the simplest factorization model of Eq. 37 and multiply the band of results obtained in ref. [1] for proton-proton total cross-section with a constant factor. This is similar to what we did in Fig. 1, except that we use the full band from Fig. 2 of ref.[1]. Let us indicate these predictions as $BN_F = BN_{protons}/330$ (F for factorization). We then compare this band with the results obtained using the BN model with photon densities, GRS and CJKL, namely the curves shown in Fig. 3, extended to $\sqrt{s_{\gamma p}} = 20\ TeV$. This comparison is shown in Fig. 5. We see that, at energies around and through the TeV region, the band obtained from σ_{tot}^{pp} falls short of what the BN model for photons (BN_γ) predicts. Other models, which enjoy factorization like the Aspen model, also remain lower than our curves. While at moderate, HERA like energies, all the three models, Aspen, BN_γ or BN_F give acceptable fits to the data, there is a difference of almost 50% among their high energy extrapolations. Thus, the first interesting conclusion from this exploration of the very high energy region is that there is a distinct difference between predictions from our BN model and those from the QCD inspired model of Block et al. (Aspen) [24], as well as from a straightforward multiplication of our band of predictions for the proton times a normalization factor.

The next interesting result from this extrapolation appears when one compares our model predictions with the fit to HERA data performed by Block and Halzen and based on a low energy parametrization of γp resonances joined with Finite Energy Sum Rules (FESR) and asymptotic $\ln^2 s$ behaviour [67]. Fig. 6 shows a band corresponding to the predictions of our model for photons (upper band) compared to BN_F (lower band), the Block and Halzen fit [67], the Aspen model of [24], and an eikonal mini-jet curve which uses the proton and pion form factors for the impact parameter distribution (FF model). The central (full) curve in the upper band corre-

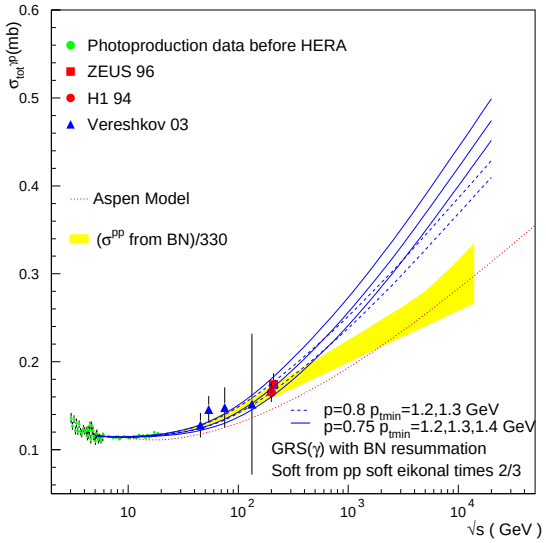

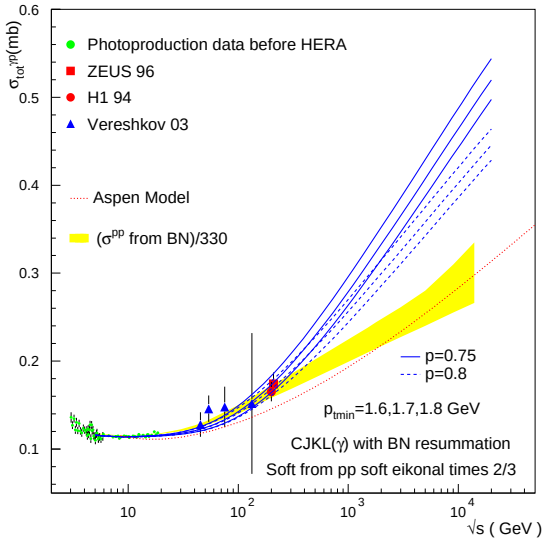

Fig. 5. Total γp cross-section with GRS and CJKL densities, compared with ref. [24] predictions and with a brute force factorization of our proton-proton results from [1].

sponds to the BN_γ model with $p_{tmin} = 1.3\,GeV, p = 0.75$ and GRS densities.

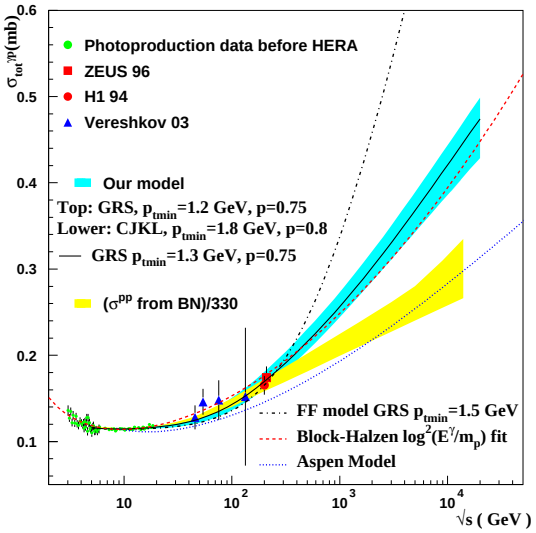

Fig. 6. Total γp cross-section with expectation from BN model using GRS and CJKL densities (upper band) for the photon, compared with the model in [24], the fit described in [67], a factorization model (lower band) and the eikonal mini-jet model without soft gluons (dot-dashes).

Fig. 6 deserves some comment. For the curves shown in this figure, the parameters have been chosen so as to reproduce the highest available accelerator data (through p_{tmin} and p values for the BN model, and through p_{tmin} for the FF model) and the low energy data, the latter through P_{had} and σ_0. As the c.m. energy increases, the model results show noticeable differences between the *hadron-like* models, Aspen and BN_F, and the photon-density model BN_γ, and much more between all of them and the eikonal mini-jet (EMM) Form Factor model. Neglecting the FF model, which we think is incomplete, we nonetheless have a remarkable difference in the very high energy range, 10 TeV and beyond. Because these predictions may impact strongly on the photon content of high energy cosmic rays [65,66], this difference does matter.

We notice that the curve, labelled Block-Halzen (BH), from [67] lies within the band of the BN_γ model. The BH curve is based on a best fit to low energy γp data, joined smoothly with a fit of high energy accelerator [12,13] and cosmic ray data [64] of the form

$$\sigma_{\gamma p} = c_0 + c_1 \log(\nu/m) + c_2 \log^2(\nu/m) + \beta_{\mathcal{P}'}/\sqrt{\nu/m} \quad (38)$$

where ν s the laboratory photon energy. There is a noticeable difference between the slope in the rising part of the cross-section between the Aspen model and the BH fit, as there is between the modelling content between all these descriptions. In our model the rise is based on the gluon densities entering the calculation of the QCD mini-jets cross-sections and on the soft gluon resummation ansätz for the impact parameter distribution. The calculation of these inputs relies on realistic PDF distributions and actual, LO, parton parton cross-section. Then, the very high energy (in the TeV region) agreement between the BH best fit based on an analytic expression and our results is an independent check of the correct physics content of the BN model. This fit confirms the inherent interest of our approach based on QCD mini-jets and soft gluon resummation.

For possible use, we report in table 1, the numerical values obtained in our model for the cross-sections shown in Fig. 6.

From a numerical point of view, the curves for the BN model for protons and photons differ because the b-distributions for protons or photons obtained in our model from $A_{BN}(q_{max}(s), b)$ differ, and they differ because the maximum momentum allowed to individual soft gluons is different. This quantity for the hard part is obtained through the kinematic constraint averaged over the quark densities and the latter are of course different for protons and photons. This is apparent from a comparison of $q_{max}(s)$ for pp [1,68] and γp : for comparable c.m. energies $q_{max}(s)$ for pp rises to higher values than the one for γp, resulting in more saturation for pp. These differences are due to the quark densities entering the averaging process defining $q_{max}(s)$: densities are a phenomenologically extracted quantity and as such it is to be expected that they reflect the different structure of the interacting particles, namely the difference between valence quarks bound in a proton and quark pairs in which the photon will split and their respective evolution.

7 Conclusions

We have applied to γp scattering an eikonal mini-jet model with soft gluon resummation developed for the proton total cross-section. The model relies on the parton structure of protons and photons and indicates a different high energy behaviour for γp relative to pp and $\bar{p}p$. We suggest that this different behaviour may be due to the different parton structure and high energy evolution properties of quarks in the proton and quarks in the photon. Furthermore, this result strengthens our confidence in the BN model as a good approximation to a QCD description of hadronic interactions in minimum bias processes.

Acknowledgments

We thank Dieter Haidt and Bernd Surrow for pointing out to us the ZEUS BPC95 data. R.G. aknowledges support from the Department of Science and Technology, India, under the J.C. Bose fellowship. G. P. thanks the Boston University Theoretical Physics group and the MIT LNS for hospitality while this work was being written. This work has been partially supported by MEC (FPA2006-05294) and Junta de Andalucía (FQM 101 and FQM 437).

Appendix A: The mini-jet cross-section

The QCD jet cross-section for the process

$$hadron_A + hadron_B \to X + jet \quad (A1)$$

is obtained by embedding the parton-parton subprocess cross-section with the given parton densities and integrating over all values of incoming parton momenta and outgoing parton transverse

Table 1. Values (in mb) for total cross-section for γp scattering evaluated in the c.m. energy of colliding particles, corresponding to the bands shown in Fig. 6.

$\sqrt{s}$ GeV	EMM with Form Factors,GRS $p_{tmin} = 1.5$ GeV	BN_γ model (upper curve) top band	BN_γ model (lower curve) top band	$BN_{proton}/330$ (upper curve) lower band	$BN_{proton}/330$ (lower curve) lower band
5	0.116	0.116	0.116	0.118	0.119
10				0.115	0.116
11.46	0.114	0.115	0.114		
48.93	0.122	0.130	0.121		
50				0.131	0.129
100				0.15	0.143
112.14	0.139	0.155	0.140		
478.74	0.238	0.228	0.203		
500				0.199	0.182
1000				0.221	0.199
1097.3	0.352	0.279	0.250		
4684.6	0.635	0.384	0.338		
5000				0.280	0.240
9000				0.310	0.255
10736.8	0.829	0.449	0.390		
14000				0.335	0.266
20000	0.985	0.499	0.429		

momentum p_t, according to the expression

$$\sigma_{\rm jet}^{AB}(s, p_{tmin}) = \int_{p_{tmin}}^{\sqrt{s}/2} dp_t \int_{4p_t^2/s}^{1} dx_1 \int_{4p_t^2/(x_1 s)}^{1} dx_2 \times \sum_{i,j,k,l} f_{i|A}(x_1, p_t^2) f_{j|B}(x_2, p_t^2) \frac{d\hat{\sigma}_{ij}^{kl}(\hat{s})}{dp_t} \quad \text{(A2)}$$

where A and B are the colliding hadrons or photons, in this case $A - proton, B - \gamma$. By construction, this cross-section depends on the particular parametrization of the DGLAP [69] evoluted parton densities, some of which do extend to very low x-values but not too high p_t^2 values. This cross-section strongly depends on the lowest p_t value on which one integrates. The term *mini-jet* was introduced long ago [30,31] to indicate all those low p_t processes which one can still expect to be QCD calculable but which are actually not observed as hard jets. p_t being the scale at which to evaluate α_s in the mini-jet cross-section calculation, one can have $p_{tmin} \approx 1 \div 2\ GeV$.

Appendix B: The calculation of $q_{max}(s)$

Simple kinematics can give the maximum transverse momentum allowed to single gluon emission in a process like

$$parton_1(x_1) + parton_2(x_2) \rightarrow gluon(k) + X(Q) \quad \text{(B1)}$$

namely

$$M(x_1, x_2, Q^2) = \frac{\sqrt{\hat{s}}}{2}(1 - \frac{Q^2}{\hat{s}}) \quad \text{(B2)}$$

with $\hat{s} = s x_1 x_2$. If X represents two jets from the outgoing parton-antiparton pair, one can use $Q^2 \approx 4p_t^2$. The calculation is simplified by introducing an average over the parton parton cross-section and integrate over all x values [56] obtaining

$$q_{\max}(s) = \frac{\sqrt{s}}{2} \frac{\int (dx_1 dx_2) \int_{z_{min}}^{1} dz \sqrt{x_1 x_2}(1-z) D(x_1, x_2)}{\int (dx_1 dx_2) \int_{z_{min}}^{1} dz D(x_1, x_2)} \quad \text{(B3)}$$

where $z_{min} = 4p_{tmin}^2/s$, D denotes the usual quark density expression

$$D(x_1, x_2) = \sum_{i,j} [f_i(x_1)/x_1][f_j(x_2)/x_2] \quad \text{(B4)}$$

and we have also assumed that the parton-parton cross-section, appearing at both numerator and denominator, can be evaluated at its maximum value, $p_t = p_{tmin}$, thus dropping out of the calculation.

References

1. A. Achilli, R. M. Godbole, A. Grau, R. Hegde, G. Pancheri and Y. Srivastava, Phys. Lett. B **659** (2008) 137 [arXiv:0708.3626 (hep-ph)].
2. For a recent review, see M. Block, Phys.Rept.**436** (2006) 71-215. e-Print: hep-ph/0606215, and references therein; M. M. Block and F. Halzen, Phys. Rev. D **73** (2006) 054022 [arXiv:hep-ph/0510238];
3. For reviews see, for example, M. Drees and R. M. Godbole, J. Phys. G **21** (1995) 1559 [arXiv:hep-ph/9508221]; M. Krawczyk, A. Zembrzuski and M. Staszel, Phys. Rep. **345** (2001) 265 [arXiv:hep-ph/0011083].
4. A. Corsetti, R. M. Godbole and G. Pancheri, Phys. Lett. B **435** (1998) 441 [arXiv:hep-ph/9807236].
5. R. M. Godbole, A. De Roeck, A. Grau and G. Pancheri, JHEP **0306** (2003) 061 [arXiv:hep-ph/0305071].
6. R. M. Godbole and G. Pancheri, Eur. Phys. J. C **19** (2001) 129 [arXiv:hep-ph/0010104].
7. V. N. Gribov, J. Exp. The. Phys. (USSR) vol. **41** (1961) p. 667. English translation JETP vol.**14** (1962) 478; V. N. Gribov and I. Ya. Pomeranchuk, Phys. Rev. Lett. **8** (1962) 343.
8. M. Block and K.Kang, Int. J. Mod. Phys. **A20** (2005) 27812794. e-Print: hep-ph/0302146; M.M. Block and A.B. Kaidalov, Phys. Rev . **D64** (2001) 076002, e-print: hep-ph/0012365.
9. J.R. Cudell, E. Martynov, G. Soyez, Nucl.Phys. **B682** (2004):391 [arXiv: hep-ph/0207196]; J. R. Cudell and O. V. Selyugin, Phys.Lett. **B662** (2008) 417 [arXiv:hep-ph/0612046].
10. C. Bourrely, J. Soffer and T.T. Wu, Mod. Phys. Lett. **A15** (2000), 9-13. [arXiv: hep-ph/9903438]
11. A. Donnachie and P. V. Landshoff, Phys. Lett. B **296** (1992) 227 [arXiv:hep-ph/9209205]; A. Donnachie and P. V. Landshoff, Phys. Lett. B **595**(2004) 393 [arXiv:hep-ph/0402081].
12. H1 Collaboration, S. Aid et al., Zeit. Phys. **C69** (1995) 27, hep-ex/9509001.
13. ZEUS collaboration, S. Chekanov et al., Nucl. Phys. **B627** (2002) 3, hep-ex/0202034.
14. R. M. Godbole, A. Grau, G. Pancheri and Y. N. Srivastava, Phys. Rev. D **72** (2005) 076001 [arXiv:hep-ph/0408355].
15. M. Froissart, Phys. Rev. **123** (1961) 1053. A. Martin, Phys. Rev. **129** (1963) 1432; Nuovo Cimento **42** (1966) 930.
16. E. Gotsman, E. Levin and U. Maor, Eur.Phys.J. **C5** (1998) 303, hep-ph/9708275.
17. L3 Collaboration, M. Acciarri, et al, **CERN-EP/2001-012**, Phys. Lett. **B519** (2001) 33 , hep-ex/0102025; OPAL Collaboration. G. Abbiendi et al., Eur. Phys. J. **C14** (2000) 199 .
18. W.-M. Yao *et al.* **Particle Data Group**, J. Phys. G **33** (2006) 1.
19. G. Arnison *et al.*, **UA1** Collaboration, Phys. Lett. **128B** (1983) 336 ; R. Battiston *et al.* **UA4** Collaboration, Phys. Lett. **B117** (1982) 126; C. Augier *et al.* **UA4/2** Collaboration, Phys. Lett. **B344** (1995) 451 ; M. Bozzo *et al.* **UA4** Collaboration, Phys. Lett. **147B** (1984) 392 ; G.J. Alner *et al.* **UA5** Collaboration, Z. Phys. **C32** (1986) 153 ; N. Amos *et. al.*, **E710** Collaboration, Phys. Rev. Lett. **68** (1992) 2433 ; C. Avila *et. al.*, **E811** Collaboration, Phys. Lett. **B445** (1999) 419; F. Abe *et. al.*, **CDF** Collaboration, Phys. Rev. **D50** (1994) 5550.
20. J.C. Collins and G.A. Ladinsky, Phys. Rev.**D43** (1991) 2847.
21. C. Amsler *et al.*, The Review of Particle Physics, Phys. Lett.**B667** (2008) 1.
22. ECFA/DESY LC Physics Working Group (E. Accomando et al.), Phys. Rep. **299** (1998) 1 [arXiv: hep-ph/9705442].
23. Y. Novoseltsev, R. Novoseltseva, G. Vereshkov, J. Phys. **G36** (2009) 025009, e-Print: arXiv:0802.0956 [hep-ph].
24. M. Block, E. Gregores, F. Halzen and G. Pancheri, Phys. Rev. **D60** (1999) 054024, e-Print: hep-ph/9809403.
25. M.M. Block, F. Halzen, T. Stanev, Phys. Rev.D **62** (2000) 077501, e-Print: hep-ph/0004232.
26. A. Grau, G. Pancheri and Y. N. Srivastava, Phys. Rev. D **60** (1999) 114020 [arXiv:hep-ph/9905228].

27. A. Corsetti, A. Grau, G. Pancheri and Y. N. Srivastava, Phys. Lett. B **382** (1996) 282 [arXiv:hep-ph/9605314].
28. H. Cheng and T. T. Wu, Phys.Rev. **186** (1969) 1611.
29. C. Bourrely, J. Soffer , T. T. Wu, Phys. Rev. D **19** (1979) 3249.
30. R. Horgan and M. Jacob, Nucl. Phys. **B179** (1981) 441.
31. G. Pancheri and C. Rubbia, Nucl. Phys. **A** (1984) 418:117C-138C.
32. D.R. Yennie, S. C. Frautschi and H. Suura, Annals Phys. **13** (1961) 379.
33. Y. I. Dokshitzer, D.I. Dyakonov and S.I. Troyan, Phys. Lett. **79B** (1978) 269.
34. G. Parisi and R. Petronzio, Nucl.Phys. **B154** (1979) 427.
35. F. Halzen, A. D. Martin, D.M. Scott, M.P. Tuite, Z. Phys. **C14** (1982) 351.
36. G. Altarelli, R.K. Ellis, M. Greco, G. Martinelli, Nucl.Phys. **B246** (1984) 12.
37. G. Curci, Mario Greco, Y. Srivastava, Nucl.Phys. **B159** (1979) 451.
38. G. Pancheri-Srivastava and Y.N. Srivastava, Phys.Rev. **D15** (1977) 2915.
39. Y.L. Dokshitzer, *Perturbative QCD Theory (includes our knowledge of α_s)*, Plenary Talk at ICHEP 1998, Vancouver, hep-ph/9812252
40. Raj Gandhi, Ina Sarcevic, Phys. Rev. **D44** (1991) 10-14.
41. R.S. Fletcher, T.K. Gaisser and F. Halzen, Phys. Lett. **B298** (1993) 442; Phys. Rev. **D45** (1992) 377-381, Erratum-ibid.**D45** (1992) 3279.
42. M. Glück, E. Reya, and A. Vogt, Z. Phys. **C53**(1992) 127; Z. Phys. **C67** (1995) 433; Eur. Phys. J. **C 5** (1998) 461.
43. A. D. Martin, R. G. Roberts, W. J. Stirling, and R. S. Thorne, Phys. Lett. **B531** (2002) 216.
44. H.L. Lai, J. Botts, J. Huston, J.G. Morfin, J.F. Owens, Jian-wei Qiu, W.K. Tung, H. Weerts, Phys.Rev. **D51** (1995) 4763.
45. M. Glück, E. Reya and A. Vogt, Phys. Rev.**D 46** (1992) 1973.
46. M. Glück, E. Reya and I. Schienbein, Phys. Rev. **D 60** (1999) 054019; Erratum, ibid **D 62** (2000) 019902.
47. F. Cornet, P. Jankowski, M. Krawczyk and A. Lorca, Phys. Rev. **D 68** (2003) 014010.
48. R.M. Godbole, A. Grau, G. Pancheri and Y.N. Srivastava, Nucl. Phys. Proc. Supp. **184** (2008) 85-90, e-Print: arXiv:0802.3367 [hep-ph].
49. L. Durand, H. Pi, Phys.Rev.**D40** (1989) 1436.
50. R. M. Godbole , G. Pancheri, Eur.Phys.J.**C 19** (2001) 129, e-Print: hep-ph/0010104.
51. *Photon total cross-sections*, R.M. Godbole, A. Grau , G. Pancheri, Y.N. Srivastava, Nucl. Phys. Proc. Suppl. **126** (2004) 94-99. Also in *Frascati 2003, The structure and interactions of the photon*, p.94-99 e-Print: hep-ph/0311211.
52. E.G.S. Luna, Phys. Lett. **B641** (2006) 171-176. e-Print: hep-ph/0608091, and references therein; E.G.S. Luna and A.A. Natale, Phys. Rev. **D 73** (2006) 074019, hep-ph/0602181.
53. J. Bartels, D. Colferai, S. Gieseke, A. Kyrieleis, Phys.Rev. **D66** (2002) 094017. e-Print: hep-ph/0208130; J. Bartels, S. Gieseke and C.F. Qiao, Phys. Rev. **D63** (2001) 056014, Erratum-ibid.**D65** (2002)079902, e-Print: hep-ph/0009102.
54. E. Etim, G. Pancheri and B. Touschek, Nuovo Cimento **51B** (1967) 276.
55. A. Nakamura, G. Pancheri, Y.N. Srivastava, Z. Phys. **C21** (1984) 243.
56. M. Greco and P. Chiappetta, Nucl. Phys. **B221** (1983) 269.
57. F.J. Yndurain, Lectures given at 17th Autumn School: *QCD: Perturbative or Nonperturbative?* (AUTUMN 99), Lisbon, Portugal, 29 Sep - 4 Oct 1999. Published in *Lisbon 1999, QCD: Perturbative or nonperturbative?* p.97-129 e-Print: hep-ph/9910399.
58. J. L. Richardson, Phys. Lett. **B82** (1979) 272. For an application to deep inelastic scattering, see K. Adel, F. Barreiro and F. J. Yndurain, Nucl. Phys.**B495** (1997) 221.
59. A.M. Polyakov, JETP Lett. **20** (1974) 194.
60. D. Haidt , *The transition from $\sigma(\gamma^* p)$ to $\sigma(\gamma p)$*, Prepared for 9th International Workshop on Deep Inelastic Scattering (DIS 2001), Bologna, Italy, 27 Apr - 1 May 2001. Published in *Bologna 2001, Deep inelastic scattering* 287-290, and refs. therein.
61. ZEUS Collaboration, J. Breitweg et al., Phys. Let. **B407** (1997) 432, DESY-97-135, hep-ex/9707025v3; ZEUS Collaboration, J. Breitweg et al., Phys. Let. **B487** (2000) 53, DESY-00-071, hep-ex/0005018v2.
62. B. Surrow, DESY-THESIS-1998-004; A. Bornheim, in the *Proceedings of the LISHEP International School on High Energy Physics, Brazil, 1998*, hep-ph/9806021.
63. ZEUS Collaboration, J. Breitweg et al., EPJC **7** (1999) 609, DESY-98-121, hep-ex/9809005v1.

64. G.M. Vereshkov, O.D. Lalakulich, Yu.F. Novoseltsev, R.V. Novoseltseva, Phys.Atom.Nucl.**66** (2003) 565-574, Yad.Fiz.**66** (2003) 591-600.
65. M. Ave, J.A. Hinton, R.A. Vazquez, A.A. Watson, E. Zas, Phys. Rev. **D67** (2003) 043005. e-Print: astro-ph/0208228; M. Ave, J.A. Hinton, R.A. Vazquez , A.A. Watson, E. Zas, Phys. Rev. **D65** (2002) 063007. e-Print: astro-ph/0110613.
66. Pierre Auger Collaboration (J. Abraham et al.). FERMILAB-PUB-07-736-A, Dec 2007. 28pp. Astropart.Phys. **29** (2008) e-Print: arXiv:0712.1147 [astro-ph].
67. M. Block and F. Halzen, Phys.Rev. **D70** (2004) 091901. e-Print: hep-ph/0405174; ibidem Phys. Rev. **D72** (2005) 036006, Erratum-ibid.**D72** (2005)039902. e-Print: hep-ph/0506031.
68. G. Pancheri, R.M. Godbole, A. Grau, Y.N. Srivastava, Acta Phys. Polon. B **38** (2007) 2979 [arXiv:hep-ph/0703174].
69. Y. L. Dokshitzer, Sov. Phys. JETP **46** (1977) 641 [Zh. Eksp. Teor. Fiz.**73** (1977) 1216]; V. N. Gribov and L. N. Lipatov, Yad. Fiz. **15** (1972) 781 [Sov. J. Nucl. Phys. **15** (1972) 438]; G. Altarelli and G. Parisi, Nucl. Phys. **B126** (1977) 298.